Acta Crystallographica Section F
Structural Biology and Crystallization Communications
ISSN 1744-3091

Expression, purification and preliminary crystallographic analysis of human thyroid hormone responsive protein

Wenzheng Zhang,[a] Wei Peng,[b] Mingzhuo Zhao,[c] Dejun Lin,[a] Zonghao Zeng,[b] Weihong Zhou[a] and Mark Bartlam[a]*

[a]Tianjin Key Laboratory of Protein Science, College of Life Sciences, Nankai University, Tianjin 300071, People's Republic of China, [b]National Laboratory of Biomacromolecules, Institute of Biophysics (IBP), Chinese Academy of Sciences, Beijing 100101, People's Republic of China, and [c]School of Physics, Hunan University of Science and Technology, Xiangtan 411201, People's Republic of China

Correspondence e-mail: bartlam@nankai.edu.cn

Received 10 March 2011
Accepted 1 June 2011

Thyroid hormone responsive protein (Thrsp, also known as Spot 14 and S14) is a carbohydrate-inducible and thyroid-hormone-inducible nuclear protein specific to liver, adipose and lactating mammary tissues. Thrsp functions to activate genes encoding fatty-acid synthesis enzymes. Recent studies have shown that in some cancers human Thrsp (hS14) localizes to the nucleus and is amplified, suggesting that it plays a role in the regulation of lipogenic enzymes during tumourigenesis. Thrsp, a member of the Spot 14 superfamily, is an acidic homodimeric protein with no sequence similarity to other mammalian gene products and its biochemical function is elusive. To shed light on the structure–function relationship of this protein, human Thrsp was crystallized. Recombinant human Thrsp (hThrsp), the N-terminally truncated human $Thrsp_{10–146}$ (hThrsp9) and their selenomethionyl (SeMet) derivatives were expressed in *Escherichia coli*, purified and crystallized using the hanging-drop vapour-diffusion method. Diffraction-quality crystals were grown at 293 K using Li_2SO_4 as a precipitant. Using synchrotron radiation, data for the hThrsp SeMet derivative, hThrsp9 and its SeMet derivative were collected to 4.0, 3.0 and 3.6 Å resolution, respectively, at 100 K. The crystals of full-length hThrsp and its SeMet derivative belonged to space group $P4_12_12$, with approximate unit-cell parameters $a = b = 123.9$, $c = 242.1$ Å, $\alpha = \beta = \gamma = 90.0^\circ$. In contrast, the crystals of the truncated hThrsp9 and its SeMet derivative belonged to space group $P2_12_12_1$, with approximate unit-cell parameters $a = 91.6$, $b = 100.8$, $c = 193.7$ Å, $\alpha = \beta = \gamma = 90.0^\circ$. A molecular-replacement solution calculated using a murine Spot 14 structure as a search model indicated the presence of six molecules per asymmetric unit, comprising three hThrsp homodimers.

1. Introduction

The thyroid hormone responsive protein (Thrsp, also known as Spot 14 and S14) is an ~17 kDa acidic (pI 4.65) protein bearing no sequence similarity to other functional motifs and with a strong propensity for homodimerization (Cunningham *et al.*, 1997; Chou *et al.*, 2007). It was first identified in 1982 as a result of its marked and rapid induction by thyroid hormone (Seelig *et al.*, 1982). The multi-layered regulation and nuclear localization of Thrsp led researchers to believe that it plays a role in tissue-specific control of metabolism in response to changing dietary and hormonal factors (Campbell *et al.*, 2003; Cunningham *et al.*, 1998; Franklyn *et al.*, 1989). Thrsp has been reported to be a homodimeric transcriptional activator that serves as a component of a tripartite complex with a 36 kDa hepatic protein in rat liver to modulate gene expression (Cunningham *et al.*, 1997). The biochemical mechanism of Thrsp is not known, but it evidently functions to transduce hormone- and nutrient-related signals to genes involved in lipid metabolism. Expression of the human Thrsp (hThrsp, hS14) gene is abundant in those tissues that are active in long-chain fatty-acid synthesis, such as the lactating mammary gland (Dozin *et al.*, 1986; Kinlaw *et al.*, 1995; Ma & Goodridge, 1992), and its localization in hepatic nuclei further suggests that it functions in the regulation of lipogenic enzyme genes (Brown *et al.*, 1997; Cunningham *et al.*, 1998; Kinlaw *et al.*, 1992; Zhu

© 2011 International Union of Crystallography
All rights reserved

et al., 2001, 2005). Furthermore, hThrsp in the cancer amplicon has been proposed as a biomarker of aggressive breast cancer (Kinlaw *et al.*, 2006; Moncur *et al.*, 1997; Taviaux *et al.*, 1997), promoting a lipogenic tumour phenotype characterized by high fatty-acid synthesis rates, elevated lipogenic enzyme levels in tumours (*e.g.* fatty-acid synthase, acetyl-CoA carboxylase and malic enzyme) and a dependence on lipogenesis for tumour-cell growth (Towle *et al.*, 1997; Kuhajda, 2000). In MCF-7 human breast-cancer cells, overexpression of hS14 decreases cell growth and induces cell death and differentiation (Sanchez-Rodriguez *et al.*, 2005).

A recent study demonstrated that hThrsp physically and functionally interacts with the thyroid receptor (TR) in the regulation of malic enzyme gene expression. The ubiquitous expression of hThrsp in various cell lines and its cell-type-dependent functions suggest that it acts as a positive or negative cofactor of the TR to regulate malic enzyme gene expression (Chou *et al.*, 2007). Similarly, its nuclear localization also suggests that hThrsp might act as a transcription cofactor in the regulation of specific genes. Chou and coworkers showed that its C-terminal region regulates the potential transactivation activity of hThrsp and is involved in the regulation of p53-dependent transactivation. hThrsp might therefore regulate the transcription and translation of p21, the p53 target gene, *via* direct interaction with the TR or other p53 coactivators such as Zac1 (zinc-finger protein which regulates apoptosis and cell-cycle arrest 1; Chou *et al.*, 2008). These studies suggest a molecular basis for a novel function of human Thrsp in TR-dependent or p53-dependent transcriptional activation of specific gene expression.

At the end of 2010, Colbert and coworkers reported the monomer structure of murine S14 and indicated the structure of the homodimer *via* crystallographic symmetry. Based on the structure of S14, they suggested a mechanism in which heterodimer formation with MIG12 attenuates the ability of MIG12 to activate ACC (Colbert *et al.*, 2010). Comparison of the amino-acid sequences of human Thrsp and mouse S14 revealed 82% identity (Fig. 1) and indicated certain differences in three antiparallel α-helices and one region (residues 77–104 of mouse S14, corresponding to 77–101 of hThrsp) that was not modelled in the structure of mouse S14. These regions may give rise to different physiological consequences for human Thrsp and mouse S14, such as the recognition of different partners. As human Thrsp is a driver and a marker of virulent breast cancer and a potential therapeutic target (Kinlaw *et al.*, 2006; Wells *et al.*, 2006), the precise structure of hThrsp will help to elucidate its precise biological mechanism and benefit the discovery of novel anticancer drugs. Therefore, in order to explore the detailed function of hThrsp, we set out to determine its three-dimensional structure. Here, we report our results on the expression, purification, crystallization and preliminary X-ray crystallographic analysis of recombinant hThrsp, the N-terminally truncated hThrsp9 and their respective SeMet derivatives.

2. Materials and methods

2.1. Gene cloning

A full-length cDNA fragment (Thrsp gene) encoding hThrsp was cloned into the expression plasmid pGEX-6P-1 vector (GE Healthcare) between the *Eco*RI and *Xho*I restriction sites. Thrsp and GST are connected by a short linker sequence containing a PreScission protease cleavage site, which after cleavage yields recombinant hThrsp with eight additional residues (GPLGSPEF) at its N-terminus (17.35 kDa and 154 amino-acid residues in total).

Oligonucleotide primers were designed to amplify the nucleotide sequence corresponding to a construct in which the nine N-terminal amino acids were deleted (hThrsp9) by polymerase chain reaction (PCR) using the above construct as a template. The primer sequences, which contained *Bam*HI and *Xho*I restriction sites (shown in bold), were th-9F, 5′-CG**GGATCC**AAGAACTGCCTGCTGACC-3′, and th-9R, 5′-CCG**CTCGAG**CTACCAAACTTGTCC-3′. The PCR product was cloned into the expression vector pGEX-6P-1 by conventional cloning methods. The recombinant hThrsp9 has an additional five residues (GPLGS) at its N-terminus (15.85 kDa and 142 amino-acid residues in total) after cleavage. The constructed plasmids were verified by DNA sequencing.

2.2. Expression and purification

Each recombinant plasmid was transformed into *Escherichia coli* strain BL21 (DE3) and transformed cells were plated onto LB plates containing 100 µg ml^{-1} ampicillin. A single colony was picked and grown overnight at 310 K in 10 ml LB medium containing 100 µg ml^{-1} ampicillin. The following day, 10 ml of the overnight culture was added to 1 l LB medium containing 100 µg ml^{-1} ampicillin. When the culture density reached an A_{600} of 0.6–0.8, induction with 1 m*M* IPTG (isopropyl β-D-1-thiogalactopyranoside) was performed and cell growth continued for 24 h at 289 K.

After harvesting by centrifugation (4000 rev min^{-1}, 30 min, 277 K), cells were resuspended in PBS buffer (140 m*M* NaCl, 2.7 m*M* KCl, 10 m*M* $Na_2HPO_4{\cdot}12H_2O$, 1.8 m*M* KH_2PO_4 pH 7.4) and then

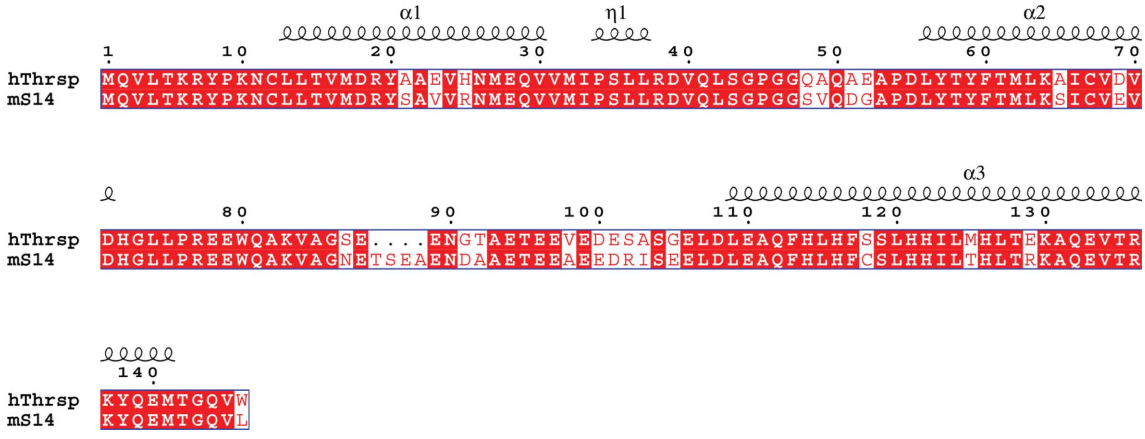

Figure 1
Sequence alignment between human Thrsp (hThrsp; NP_003242.1) and mouse Spot 14 (mS14; NP_033407.1). The numbering above the alignment corresponds to the hThrsp sequence. Secondary-structure elements for the mouse Spot 14 structure are labelled.

sonicated. After centrifugation at 18 000 rev min^{-1} for 30 min at 277 K, the clarified supernatant was passed through a glutathione-Sepharose 4B column (equilibrated with PBS buffer). The GST-fusion protein-bound column was washed with ten column volumes of PBS buffer. The GST-fusion proteins were cleaved by PreScission protease overnight at 277 K in cleavage buffer (50 m*M* Tris–HCl,

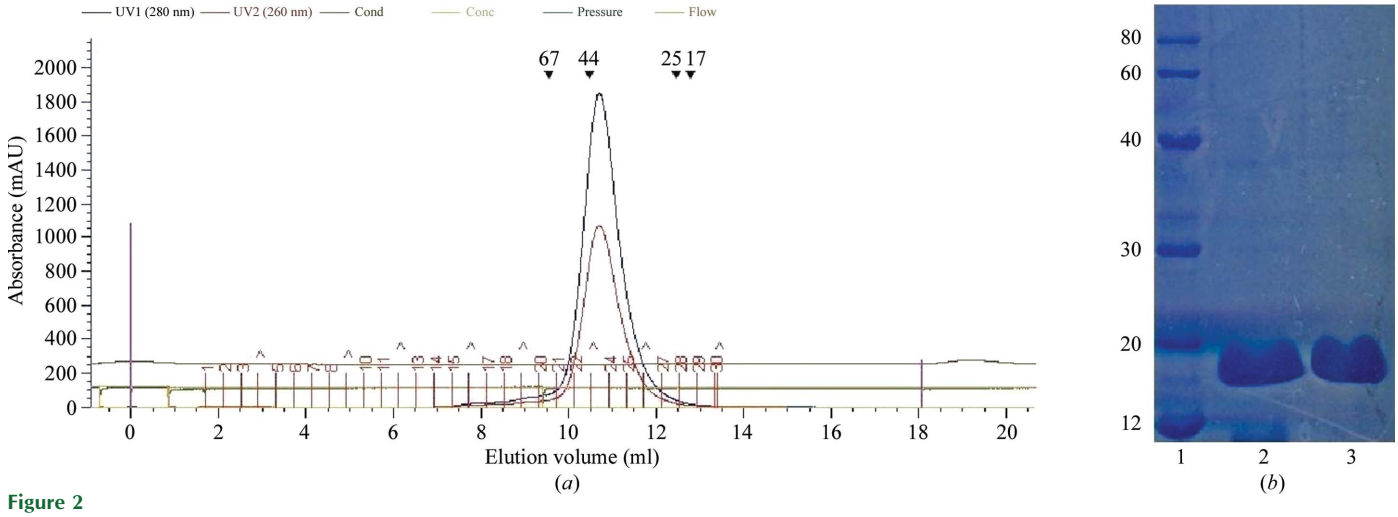

Figure 2
(*a*) The purification profile of hThrsp9 on a Superdex 75 HR 10/30 (GE Healthcare) column. The elution profile of hThrsp9 is shown together with the elution positions of some standard proteins. Arrows indicate the positions of the standard proteins (masses in kDa are indicated above the arrows): albumin (67 kDa), ovalbumin (44 kDa), chymotrypsin (25 kDa) and myoglobulin (17 kDa) at 9.6, 10.5, 12.4 and 12.7 ml, respectively. (*b*) SDS–PAGE of purified hThrsp9. Lane 1, markers (labelled in kDa); lane 2, the purified hThrsp9 used for crystallization; lane 3, hThrsp9 crystals.

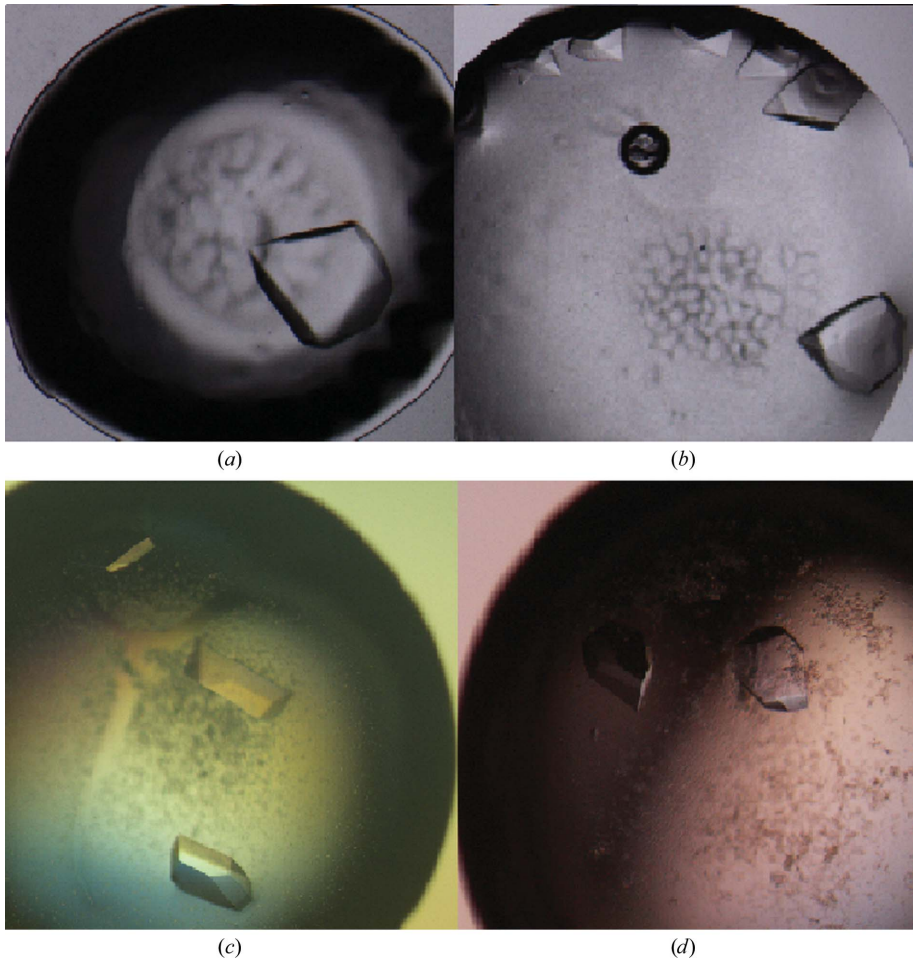

Figure 3
(*a*) Typical crystals of native human Thrsp (hThrsp; approximate dimensions 0.2 × 0.2 × 0.3 mm). (*b*) Typical crystals of SeMet hThrsp (approximate dimensions 0.1 × 0.1 × 0.2 mm). (*c*) Typical crystals of N-terminally truncated human Thrsp (hThrsp9; approximate dimensions 0.15 × 0.15 × 0.25 mm). (*d*) Typical crystals of SeMet hThrsp9 (approximate dimensions 0.1 × 0.1 × 0.2 mm).

Table 1
Data-collection and processing statistics.

Values in parentheses are for the highest resolution shell.

	hThrsp	hThrsp9 (human Thrsp$_{10–146}$)	
Data set	SeMet (peak)	Native	SeMet (peak)
Space group	$P4_12_12/P4_32_12$	$P2_12_12_1$	$P2_12_12_1$
Unit-cell parameters (Å, °)	$a = b = 123.9$, $c = 242.1$, $\alpha = \beta = \gamma = 90.0$	$a = 91.59$, $b = 100.76$, $c = 193.74$, $\alpha = \beta = \gamma = 90.0$	$a = 90.46$, $b = 100.87$, $c = 186.38$, $\alpha = \beta = \gamma = 90.0$
Wavelength (Å)	0.97984	0.97947	0.97900
Resolution (Å)	4.00 (4.14–4.00)	3.00 (3.05–3.00)	3.60 (3.66–3.60)
Total observations	224685	3720878	1702547
Unique reflections	16600	36669	20441
Data completeness (%)	99.8 (98.9)	99.4 (98.8)	97.2 (89.2)
R_{merge}† (%)	0.098 (0.492)	0.095 (0.487)	0.093 (0.468)
$\langle I/\sigma(I)\rangle$	23.49 (3.18)	20.40 (3.26)	31.90 (3.29)
Multiplicity	13.6 (10.2)	11.4 (9.5)	6.2 (5.8)

† $R_{merge} = \sum_{hkl}\sum_i |I_i(hkl) - \langle I(hkl)\rangle| / \sum_{hkl}\sum_i I_i(hkl)$, where $I_i(hkl)$ is the intensity of the ith observation of reflection hkl and $\langle I(hkl)\rangle$ is the mean intensity of the reflections.

150 m*M* NaCl, 1 m*M* DTT, 1 m*M* EDTA pH 8.0). The target protein (hThrsp or hThrsp9) was then eluted with buffer *A* (25 m*M* Tris–HCl, 150 m*M* NaCl pH 8.0) and loaded onto a Mono Q (GE Healthcare) ion-exchange chromatography column run in buffer *A*. After washing away the unbound protein with two bed volumes, a linear gradient of 0.15–1 *M* NaCl in the same buffer was applied. The target protein was further purified by gel filtration on a Superdex 75 HR 10/30 (GE Healthcare) column run in 25 m*M* Tris–HCl pH 8.0, 150 m*M* NaCl (see Fig. 2*a*). The elution profile of hThrsp9 was very similar to that of hThrsp on a Superdex 75 HR 10/30 column. The purity of the proteins was then analyzed on SDS–PAGE (better than 95% purity) and was judged to be suitable for crystallization (see Fig. 2*b*).

SeMet-labelled (SeMet) hThrsp was also expressed in *E. coli* strain BL21 (DE3). After overnight incubation in LB medium containing 100 µg ml^{-1} ampicillin, the cells were diluted with adaptive medium (20% LB medium, 80% M9 medium) and grown at 310 K to an OD_{600} of 0.6–0.8. The cells were harvested and resuspended in M9 medium, transferred into restrictive medium [5%(*w*/*v*) glucose] and grown to an OD_{600} of 0.6–0.8 before induction. SeMet at 60 mg l^{-1}, lysine, threonine and phenylalanine at 100 mg l^{-1}, leucine, isoleucine and valine at 50 mg l^{-1} and 1 m*M* IPTG were added and incubation was continued at 289 K for about 24 h. The cells were harvested and SeMet hThrsp was purified and crystallized using the same method as used for the native protein, except for the addition of a reducing environment provided by 5 m*M* DTT and 0.5 m*M* EDTA. The expression and purification and crystallization of SeMet hThrsp9 were similar to those of SeMet hThrsp. Incorporation of selenium was confirmed by mass-spectrometric analysis.

2.3. Crystallization

Purified hThrsp was exchanged into crystallization buffer (25 m*M* Tris–HCl pH 8.0, 50 m*M* NaCl) and concentrated to 20–30 mg ml^{-1} using a 5K ultrafiltration tube (Millipore). Crystallization experiments were performed at 293 K using the hanging-drop vapour-diffusion method. Preliminary crystallization trials were carried out manually using commercially available sparse-matrix screens including Crystal Screen, Index and SaltRx kits from Hampton Research, Wizard kits I and II from Emerald BioSystems and AmSO4, MPDs and Nucleix from Qiagen. Each drop was formed by mixing 1 µl protein solution and 1 µl reservoir solution and was allowed to equilibrate *via* vapour diffusion over 200 µl reservoir solution. Crystals of recombinant hThrsp were obtained using several conditions. After optimization, the best crystals were obtained from 0.95–1.05 *M* Li_2SO_4, 0.05 *M* sodium cacodylate trihydrate pH 6.0, 0.02 *M* $MgCl_2$. Crystals (0.2 × 0.2 × 0.3 mm in size; Fig. 3) were obtained in about one week. The purified SeMet derivative was concentrated to 15–30 mg ml^{-1}. Crystallization trials were set up based on the optimum conditions used for the native protein.

After gel filtration, purified hThrsp9 was concentrated to 20–30 mg ml^{-1} using a 5K ultrafiltration tube. The best crystals of hThrsp9 were obtained from a similar crystallization condition to that observed for hThrsp: 0.95–1.0 *M* Li_2SO_4, 0.1 *M* MES pH 5.0, 0.02 *M* $MgCl_2$, 0.1 *M* KCl. Crystals (0.15 × 0.15 × 0.25 mm in size; Fig. 3) appeared in 2–3 weeks and grew to their full size within 1–2 months. Meanwhile, purified SeMet hThrsp9 was concentrated to 5–10 mg ml^{-1} and crystallized based on the optimum conditions for the hThrsp9 crystals.

2.4. Data collection and processing

The diffraction quality of native hThrsp crystals was similar to that of its SeMet-derivative crystals. Data were collected from a single SeMet hThrsp crystal at the peak (λ_1; 0.97984 Å) wavelength to 4 Å resolution on beamline BL-17A under cryoconditions at the Photon Factory (Tsukuba, Japan). Data were also collected from a single SeMet hThrsp9 crystal at the peak (λ_1; 0.97900 Å) wavelength to 3.6 Å resolution on beamline BL-5A of the Photon Factory using an ADSC Quantum 315 CCD detector. Native data were also collected from an hThrsp9 crystal to 3.0 Å resolution on beamline BL17U of the Shanghai Synchrotron Radiation Facility (SSRF, China). Fig. 4 shows a typical diffraction pattern of SeMet hThrsp or hThrsp9 crystals.

During data collection, the crystals were flash-cooled to 100 K using a Cryostream (Oxford Cryosystems) in a cryoprotectant that was prepared by adding 20% glycerol to the mother liquor. Data processing and scaling were performed with the *HKL*-2000 package (Otwinowski & Minor, 1997). Data-collection statistics are reported in Table 1.

3. Results and discussion

Based on the results of size-exclusion chromatography using a Superdex 75 HR 10/30 column (see Fig. 2) and related reports (Cunningham *et al.*, 1997; Chou *et al.*, 2007; Colbert *et al.*, 2010), both hThrsp9 and hThrsp exist as homodimers in solution. At the time, no similar structures to hThrsp were available in the Protein Data Bank (PDB). As the sequence of hThrsp included six methionines, we

therefore opted to construct a SeMet-derivative protein to facilitate structure determination by the multiple/single-wavelength anomalous dispersion (MAD/SAD) method.

In order to optimize the crystallization conditions for hThrsp and its SeMet-derivative crystals following our initial screen, we varied a number of parameters, including the precipitant, buffer pH, salt, protein concentration and temperature and the use of additives, detergents and seeding. However, the diffraction resolution was not markedly improved. Finally, data to 4 Å resolution were collected from a SeMet hThrsp crystal using synchrotron radiation. The unit-cell parameters were determined to be $a = b = 123.9$, $c = 242.1$ Å, $\alpha = \beta = \gamma = 90.0^\circ$ in space group $P4_12_12$ or $P4_32_12$. Data-collection statistics from a SeMet-derivative crystal are shown in Table 1. Based on the Matthews coefficient (Matthews, 1968), we estimated there to be 12 molecules in the asymmetric unit, with a Matthews coefficient (V_M) of 2.33 Å^3 Da^{-1} and an estimated solvent content of 47%.

In order to solve the structure and thus elucidate the precise mechanism of human Thrsp, we truncated the nine N-terminal amino acids to form a new protein construct (hThrsp9) based on the results of secondary-structure prediction using the *ExPASy* proteomics server (http://expasy.org). It was anticipated that truncating the disordered N-terminal fragment of hThrsp would result in more compact or regular packing within the crystals. The hThrsp9 construct was thus expressed, purified and crystallized, together with its SeMet derivative, following the same protocol as used for the full-length hThrsp. As a result, native data from the hThrsp9 crystal and peak-wavelength data from the SeMet hThrsp9 crystal were collected using synchrotron radiation. Data sets were indexed and processed with

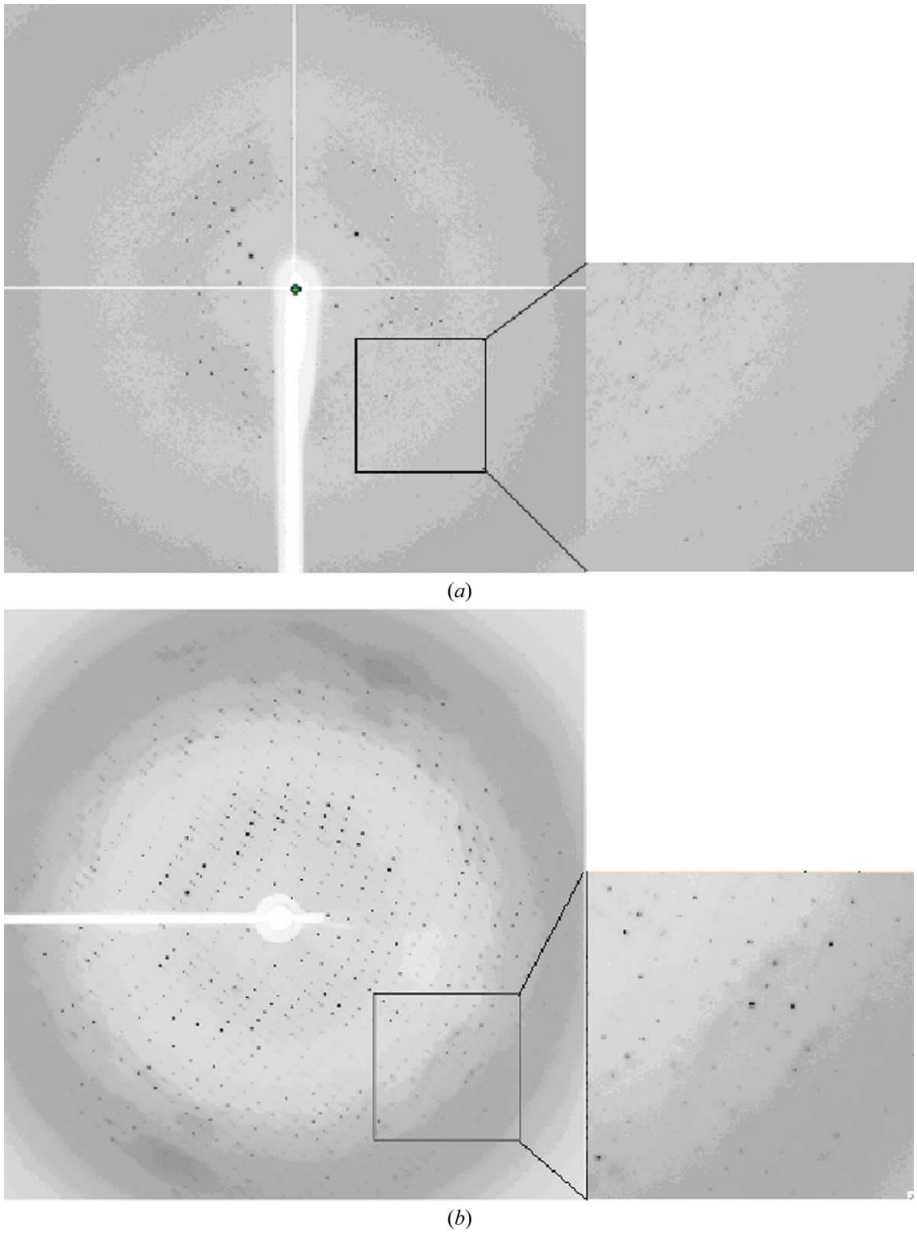

Figure 4
(*a*) A typical diffraction pattern of SeMet hThrsp crystals diffracting to 4.0 Å resolution. The diffraction image was collected on an ADSC Quantum 270 CCD detector with a crystal-to-detector distance of 392.4 mm. The oscillation range was 0.5°. An enlarged image of the area indicated is shown on the right. (*b*) A typical diffraction pattern of hThrsp9 crystals diffracting to 3.0 Å resolution. The diffraction image was collected on a MAR CCD 245 image-plate detector with a crystal-to-detector distance of 250.0 mm. The oscillation range was 0.5°. An enlarged image of the area indicated is shown on the right.

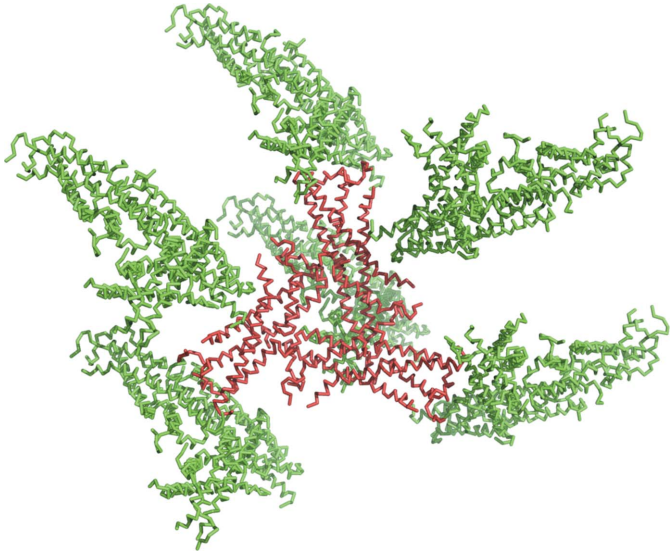

Figure 5
Crystal packing for the molecular-replacement solution of hThrsp9 (viewed down the threefold symmetry axis). The molecular-replacement solution of six hThrsp9 molecules (three homodimers) is shown in red. Symmetry-related molecules are shown in green.

HKL-2000 (Otwinowski & Minor, 1997). The native and SeMet-derivative hThrsp9 crystals belonged to space group $P2_12_12_1$, with approximate unit-cell parameters a = 91.6, b = 100.8, c = 193.7 Å, $\alpha = \beta = \gamma = 90.0^\circ$. Matthews coefficient analysis again suggested that there were 12 molecules per asymmetric unit, with a V_M (Matthews, 1968) of 2.35 Å^3 Da^{-1} and a solvent content of 48%. Data-collection statistics are summarized in Table 1.

While we were in the process of further optimizing the crystals and determining the structure by MAD/SAD phasing, the crystal structure of another member of the Spot 14 family, mouse S14 (PDB entry 3ont), was determined and reported by Colbert *et al.* (2010). Mouse S14 was crystallized in space group *I*432 with a single monomer in the asymmetric unit and a homodimer was inferred from crystallographic symmetry. Given that the amino-acid sequence identity between hThrsp and mouse S14 is 82%, we therefore attempted to determine the crystal structure of hThrsp9 by the molecular-replacement method using the structure of the mouse S14 monomer as a search model. A molecular-replacement solution was found in *Phaser* with six molecules per asymmetric unit comprising three homodimers and corresponding to a Matthews coefficient V_M of 4.70 Å^3 Da^{-1} and a solvent content of 74%. An analysis of the molecular-replacement solution showed loose packing of the hThrsp9 molecules (Fig. 5). This solution is consistent with the self-rotation function calculated using *MOLREP*, which shows threefold ($\chi = 120^\circ$) and twofold ($\chi = 180^\circ$) axes but no substantial peaks in the $\chi = 60^\circ$ section indicative of sixfold symmetry (data not shown). After initial refinement of the molecular-replacement solution, the working and free R factors were reduced from 49.3% and 48.3% to 33.2% and 38.5%, respectively.

The unexpected high solvent content of 74% should help to account for the consistently poor diffraction of hThrsp and hThrsp9 crystals. Although rare, there have been cases in which a structure has been determined from crystals with unusually high solvent content. For example, the diffraction by tetragonal crystals of human serum albumin only reaches a maximum resolution of 3.0 Å owing to their high solvent content of 77% and loose packing in the crystal lattice (Sugio *et al.*, 1999). Further refinement of the hThrsp9 structure is under way and will be reported elsewhere.

We would like to give special acknowledgement to Zihe Rao for valuable guidance and we thank Xuemei Li, Wenlong Wang, Quan Wang, Yi Han and Jianhui Li for technical instructions and assistance with data collection. We also thank the staff members of KEK and SSRF for assistance during data collection. This work was supported by the China Postdoctoral Science Foundation (grant No. 20100470799) and the Ministry of Science and Technology '973' Project (grant No. 2007CB914301).

References

Brown, S. B., Maloney, M. & Kinlaw, W. B. (1997). *J. Biol. Chem.* **272**, 2163–2166.
Campbell, M. C., Anderson, G. W. & Mariash, C. N. (2003). *Endocrinology*, **144**, 5242–5248.
Chou, W.-Y., Cheng, Y.-S., Ho, C.-L., Liu, S.-T., Liu, P.-Y., Kuo, C.-C., Chang, H.-P., Chen, Y.-H., Chang, G.-G. & Huang, S.-M. (2007). *Biochem. Biophys. Res. Commun.* **357**, 133–138.
Chou, W.-Y., Ho, C.-L., Tseng, M.-L., Liu, S.-T., Yen, L.-C. & Huang, S.-M. (2008). *Int. J. Biochem. Cell Biol.* **40**, 1826–1834.
Colbert, C. L., Kim, C.-W., Moon, Y.-A., Henry, L., Palnitkar, M., McKean, W. B., Fitzgerald, K., Deisenhofer, J., Horton, J. D. & Kwon, H. J. (2010). *Proc. Natl Acad. Sci. USA*, **107**, 18820–18825.
Cunningham, B. A., Maloney, M. & Kinlaw, W. B. (1997). *Endocrinology*, **138**, 5184–5188.
Cunningham, B. A., Moncur, J. T., Huntington, J. T. & Kinlaw, W. B. (1998). *Thyroid*, **8**, 815–825.
Dozin, B., Magnuson, M. A. & Nikodem, V. M. (1986). *J. Biol. Chem.* **261**, 10290–10292.
Franklyn, J. A., King, S., Ahlquist, J. A. & Sheppard, M. C. (1989). *Acta Endocrinol.* **121**, 383–388.
Kinlaw, W. B., Church, J. L., Harmon, J. & Mariash, C. N. (1995). *J. Biol. Chem.* **270**, 16615–16618.
Kinlaw, W. B., Quinn, J. L., Wells, W. A., Roser-Jones, C. & Moncur, J. T. (2006). *Endocrinology*, **147**, 4048–4055.
Kinlaw, W. B., Tron, P. & Friedmann, A. S. (1992). *Endocrinology*, **131**, 3120–3122.
Kuhajda, F. P. (2000). *Nutrition*, **16**, 202–208.
Ma, X. J. & Goodridge, A. G. (1992). *Nucleic Acids Res.* **20**, 4997–5002.
Matthews, B. W. (1968). *J. Mol. Biol.* **33**, 491–497.
Moncur, J. T., Park, J. P., Maloney, M., Mohandas, T. K. & Kinlaw, W. B. (1997). *Cytogenet. Cell Genet.* **78**, 131–132.
Otwinowski, Z. & Minor, W. (1997). *Methods Enzymol.* **276**, 307–326.
Sanchez-Rodriguez, J., Kaninda-Tshilumbu, J. P., Santos, A. & Perez-Castillo, A. (2005). *Biochem. J.* **390**, 57–65.
Seelig, S., Jump, D. B., Towle, H. C., Liaw, C., Mariash, C. N., Schwartz, H. L. & Oppenheimer, J. H. (1982). *Endocrinology*, **110**, 671–673.
Sugio, S., Kashima, A., Mochizuki, S., Noda, M. & Kobayashi, K. (1999). *Protein Eng.* **12**, 439–446.
Taviaux, S., Planells, R., Gastaldi, M., Torresani, J. & Grillasca, J. P. (1997). *Cytogenet. Cell Genet.* **76**, 219–220.
Towle, H. C., Kaytor, E. N. & Shih, H.-M. (1997). *Annu. Rev. Nutr.* **17**, 405–433.
Wells, W. A., Schwartz, G. N., Morganelli, P. M., Cole, B. F., Gibson, J. J. & Kinlaw, W. B. (2006). *Breast Cancer Res. Treat.* **98**, 231–240.
Zhu, Q., Anderson, G. W., Mucha, G. T., Parks, E. J., Metkowski, J. K. & Mariash, C. N. (2005). *Endocrinology*, **146**, 3343–3350.
Zhu, Q., Mariash, A., Margosian, M. R., Gopinath, S., Fareed, M. T., Anderson, G. W. & Mariash, C. N. (2001). *Endocrinology*, **142**, 4363–4370.